SHORT COMMUNICATION

Modeling Loop Reorganization Free Energies of Acetylcholinesterase: A Comparison of Explicit and Implicit Solvent Models

Mark A. Olson
Department of Cell Biology and Biochemistry, USAMRIID, Frederick, Maryland

ABSTRACT **The treatment of hydration effects in protein dynamics simulations varies in model complexity and spans the range from the computationally intensive microscopic evaluation to simple dielectric screening of charge-charge interactions. This paper compares different solvent models applied to the problem of estimating the free-energy difference between two loop conformations in acetylcholinesterase. Molecular dynamics (MD) simulations were used to sample potential energy surfaces of the two basins with solvent treated by means of explicit and implicit methods. Implicit solvent methods studied include the generalized Born (GB) model, atomic solvation potential (ASP), and the distance-dependent dieletric constant. By using the linear response approximation (LRA), the explicit solvent calculations determined a free-energy difference that is in excellent agreement with the experimental estimate, while rescoring the protein conformations with GB or the Poisson equation showed inconsistent and inferior results. While the approach of rescoring conformations from explicit water simulations with implicit solvent models is popular among many applications, it perturbs the energy landscape by changing the solvent contribution to microstates without conformational relaxation, thus leading to non-optimal solvation free energies. Calculations applying MD with a GB solvent model produced results of comparable accuracy as observed with LRA, yet the electrostatic free-energy terms were significantly different due to optimization on a potential energy surface favored by an implicit solvent reaction field. The simpler methods of ASP and the distance-dependent scaling of the dielectric constant both produced considerable distortions in the protein internal free-energy terms and are consequently unreliable. Proteins 2004;57:645–650.**

Key words: molecular dynamics; hydration; generalized Born; Poisson equation; atomic solvation potential; dielectric screening

INTRODUCTION

The population shift of enzymes from their native to functional non-native macrostates during complex formation is a measure of substrate specificity. The effect of conformational selection is nicely illustrated by the X-ray crystal structure of the reaction of acetylcholinesterase (AChE) from *Torpedo californica* with the inhibitor di*iso*propylphosphorofluor*i*date (DFP).[1] Structural changes take place in the acyl loop pocket of residues 287–290, showing the backbone displaced by roughly 5 Å. Comparison of experimental reversible dissociation constants measured for a variety of inhibitors of differing molecular size[1,3–7] suggests that the free energy penalty for loop displacement is on the order of 4 kcal/mol.

Central to the problem of modeling binding affinities, the calculation of structural reorganization is essential to reliable and accurate predictions of complex formation.[8,9,11] The experimental observation of significant loop movement in the acyl pocket offers an excellent benchmark for testing different methodological approaches to computational analysis of protein structures. This article explores the application of different solvent models of varying resolution in the calculation of the free energy difference between the conformational loop captured in the DFP-reacted macrostate and native. Molecular dynamics (MD) simulations were carried out with explicit treatment of solvent and the free energy of hydration estimated by application of linear response approximation (LRA). The hydrophobic term was calculated from a molecular surface area (SA) model. An alternative and currently popular approach was also applied of reevaluating the MD trajectory by removing the explicit solvent and scoring the

Contract/grant sponsor: U.S. Army Medical Research & Materiel Command

Contract/grant number: U.S. Army Medical Research and Materiel Command Project number RIID 02-4-1R-069

Correspondence to: Mark A. Olson, Department of Cell Biology and Biochemistry, USAMRIID, 1425 Porter Street, Frederick, MD 21702. E-mail: molson@ncifcrf.gov.

Received 5 April 2004; Revised 30 June 2004; Accepted 5 July 2004

Published online 12 October 2004 in Wiley InterScience (www.interscience.wiley.com). DOI: 10.1002/prot.20294

Report Documentation Page

Form Approved
OMB No. 0704-0188

1. REPORT DATE	2. REPORT TYPE	3. DATES COVERED
12 OCT 2004	**N/A**	**-**

4. TITLE AND SUBTITLE	5a. CONTRACT NUMBER
Modeling loop reorganization free energies from inhibitor binding to acetylcholinesterase: a comparison of explicit and implicit solvent models, Proteins: Structure, Function, and Bioinformatics	5b. GRANT NUMBER
	5c. PROGRAM ELEMENT NUMBER
6. AUTHOR(S) **Olson, MA**	5d. PROJECT NUMBER
	5e. TASK NUMBER
	5f. WORK UNIT NUMBER
7. PERFORMING ORGANIZATION NAME(S) AND ADDRESS(ES) **United States Army Medical Research Institute of Infectious Diseases, Fort Detrick, MD**	8. PERFORMING ORGANIZATION REPORT NUMBER **RPP-04-268**
9. SPONSORING/MONITORING AGENCY NAME(S) AND ADDRESS(ES)	10. SPONSOR/MONITOR'S ACRONYM(S)
	11. SPONSOR/MONITOR'S REPORT NUMBER(S)

12. DISTRIBUTION/AVAILABILITY STATEMENT
Approved for public release, distribution unlimited

13. SUPPLEMENTARY NOTES
The original document contains color images.

14. ABSTRACT
The treatment of hydration effects in protein dynamics simulations varies in model complexity and spans the range from the computationally intensive microscopic evaluation to simple dielectric screening of charge-charge interactions. This paper compares different solvent models applied to the problem of estimating the free-energy difference between two loop conformations in acetylcholinesterase. Molecular dynamics (MD) simulations were used to sample potential energy surfaces of the two basins with solvent treated by means of explicit and implicit methods. Implicit solvent methods studied include the generalized Born (GB) model, atomic solvation potential (ASP), and the distance-dependent dieletric constant. By using the linear response approximation (LRA), the explicit solvent calculations determined a free-energy difference that is in excellent agreement with the experimental estimate, while rescoring the protein conformations with GB or the Poisson equation showed inconsistent and inferior results. While the approach of rescoring conformations from explicit water simulations with implicit solvent models is popular among many applications, it perturbs the energy landscape by changing the solvent contribution to microstates without conformational relaxation, thus leading to non-optimal solvation free energies. Calculations applying MD with a GB solvent model produced results of comparable accuracy as observed with LRA, yet the electrostatic free-energy terms were significantly different due to optimization on a potential energy surface favored by an implicit solvent reaction field. The simpler methods of ASP and the distance-dependent scaling of the dielectric constant both produced considerable distortions in the protein internal free-energy terms and are consequently unreliable.

15. SUBJECT TERMS
computer modeling, free energy, acetylcholinesterase, explicit solvation, implicit

16. SECURITY CLASSIFICATION OF:			17. LIMITATION OF ABSTRACT	18. NUMBER OF PAGES	19a. NAME OF RESPONSIBLE PERSON
a. REPORT **unclassified**	b. ABSTRACT **unclassified**	c. THIS PAGE **unclassified**	**SAR**	**6**	

Standard Form 298 (Rev. 8-98)
Prescribed by ANSI Std Z39-18

conformations with either a finite-difference Poisson (FDP) technique or a generalized Born (GB) model. A third approach was investigated by performing a MD calculation with solvent treated implicitly with a GB model. Finally, an atomic solvation potential (ASP) and a distance-dependent dielectric constant model were applied as further implicit solvent schemes in MD simulations.

While there is extensive literature on GB and FDP applications, the accuracy of these models still remains uncertain. An overall contrast of different solvent-modeling techniques is much needed for an assessment of not only of the accuracy in predicting thermodynamic differences between conformational states but also modeling the correct physics underlying the differences.

METHODS

Structural reorganization between two protein loop conformations (denoted as P and P^*) located in different basins can be described by the reaction

$$P \overset{\Delta G}{\rightleftharpoons} P^* \tag{1}$$

where ΔG is the free energy difference of the protein and solvent system. The free energy $G(\xi)$ for a macrostate ξ is[12]

$$G_{\text{macro}}(\xi) = -k_B T \ln \Omega = G_{\text{micro}}(\xi) - TS_{\text{conf}}(\xi), \tag{2}$$

where Ω is the partition function, G_{micro} is the free energy of a single loop conformation taken to be the most probable microstate in ξ, S_{conf} is the conformational entropy, and $k_B T$ is the Boltzmann constant and absolute temperature.

To determine G_{micro}, we partition the free energy for each conformation into separate contributions; for example, conformation P gives

$$G^P_{\text{micro}} = E^P_{\text{int}} + G^P_{\text{solv}} + G^P_{\text{cav}}, \tag{3}$$

where E_{int} is the internal energy of the protein, G_{solv} is the solvation term and G_{cav} is the cavitation free energy given by

$$G^P_{\text{cav}} = \sum_i \gamma_i A^P_i \tag{4}$$

where for atom i, γ_i is the surface tension and A_i is the molecular surface area. The internal energy component is determined from

$$E^P_{\text{int}} = E^P_{\text{local}} + E^P_{\text{vdW}} + W^P_{\text{ele}}, \tag{5}$$

where E_{local} is the bonded and torsional terms defined by a given force field, E_{vdW} is van der Waals (vdW) intraprotein interactions, and W_{ele} is the energetic cost of creating the charge distribution in an environment of unit dielectric.

Solvent effects are modeled as the sum of non-electrostatic and electrostatic interaction contributions

$$G^P_{\text{solv}} = G^P_{\text{s,ele}} + G^P_{\text{s,vdW}}, \tag{6}$$

determined for each microstate. From explicit solvent calculations, the free energy of solvation can be estimated from the LRA (see, e.g., ref. 9)

$$G^P_{\text{solv}} = \alpha(\langle U^P_{\text{s,ele}}\rangle_P + \langle U^P_{\text{s,ele}}\rangle_{P'}) + \beta\langle U^P_{\text{s,vdW}}\rangle_P \tag{7}$$

where U is the potential energy surface of non-bonded interactions between the protein in conformation P and solvent, $\langle\ldots\rangle_P$ is the ensemble average over charged P microstates, and $\langle\ldots\rangle_{P'}$ is the average over uncharged P', and α and β are scaling constants. The form of eq. (7) can be approximated by noting that the solvent in the uncharged P' state does not experience the charge distribution of the solute,[9,10] thus setting the term $\langle U^P_{\text{s,ele}}\rangle_{P'}$ to zero.

Alternatively to LRA, loop conformations from explicit solvent simulations can be rescored via either GB or FDP after removal of water. A computationally more tractable approach to explicit water calculations is the implicit solvent schemes of MD-GB/SA and ASP, or simpler methods of linear distance-dependent dielectric constants.

The conformational entropy in macrostate ξ given by eq. (2) can be estimated in the quasi-harmonic approximation calculated from the covariance fluctuation matrix $\mathbf{C}$:[13–17]

$$\mathbf{C}^P_{ij} = \langle(\mathbf{x}^P_i - \langle\mathbf{x}^P_i\rangle)(\mathbf{x}^P_j - \langle\mathbf{x}^P_j\rangle)\rangle_\xi, \tag{8}$$

where the values of $\mathbf{x}$ are atomic coordinates of microstates of P sampled from ξ. Frequencies υ_i of the normal modes are defined by the eigenvalues λ_i

$$(2\pi\upsilon_i)^2 = k_B T/\lambda_i, \tag{9}$$

and the entropy $S_{\text{conf}}(\xi)$ is approximated by[13]

$$TS_{\text{conf}}(\xi) = \sum_i -k_B T \ln[1 - \exp(-h\upsilon_i / k_B T)] + h\upsilon_i / [1 - \exp(-h\upsilon_i / k_B T)] \tag{10}$$

where h is Planck's constant.

Calculation of native microstates started with the Cartesian coordinates taken from the crystallographic PDB file 2ACE. Crystallographic waters were ignored in all calculations. The alternative loop conformation (residues 287–290) was taken from the 2DFP structure. To model a common structure differing only in the loop conformation, the alternative loop was built into 2ACE by substitution of the native and optimized by a Monte Carlo simulation.[18] Figure 1 shows a superposition of native loop and the reorganized loop. Backbone geometries of the two conformations differ by the 180° reorientation of the plane of the peptide bond between Ile-287 and Phe-288. The peptide hydrogen of Phe-288 is pointing inside the active-site gorge for the native conformation and outside the gorge upon displacement. Because of this reorientation, the native loop is designated the 'in' conformation and the alternative conformation as the 'out' conformation.

To determine ΔG_{macro} for 'in' $\rightarrow$ 'out' loop reorganization, the computational approach builds upon a previous simulation study, which showed that no dynamic connectivity exists between the two macrostates.[18] Moreover, both states exhibit Gaussian-like probability distribution functions along the normal modes.[18] Because of the deep

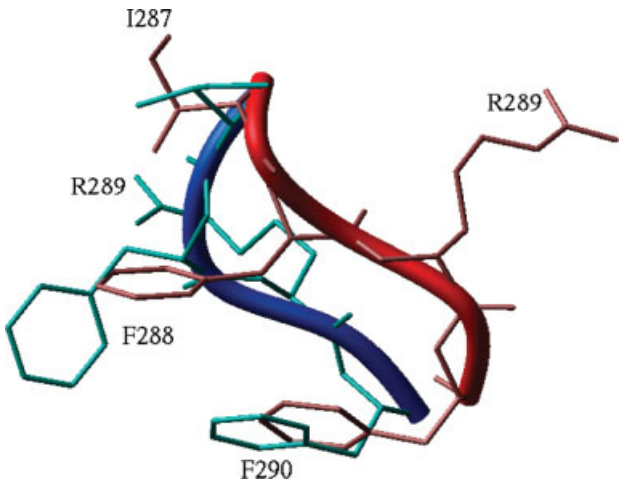

Fig. 1. Molecular illustration of loop reorganization in acetylcholinesterase resulting from inhibitor reaction.[1] The 'in' loop conformation (residues 287–290) is shown in blue and the 'out' conformation in red.

funnel-like basins, the ensemble of protein configurations for the 'out' loop with and without DFP is nearly identical, and this allows the application of a two-state simulation model without modeling the bound inhibitor. Without the advantage of funnels, either structural constraints are required on the protein configuration to remain in the 'out' state or bound DFP must be modeled and a computational strategy implemented similar to that described by Warshel and coworkers,[8,9] among others.[11] Alternatively, the transition between the two states can be described in terms of a binding cycle of different ligands that bind the native conformation versus the non-native.[19] The advantage of this latter approach when developed in a LRA framework is the need to only model the change in ligand–protein interaction as a reasonable approximation for the corresponding change in the interaction between different protein conformations.[19]

MD simulations were performed with the Tinker program[20] using the AMBER94 force field.[21] The simulation volume was constructed from a shell of residues a within 12 Å distance of residues 287–290 in the starting structures, giving a total of 127 active residues. The remaining residues were tethered to their initial positions. Explicit water calculations of the protein active region contained a 20 Å shell of solvent (1675 waters) modeled by the TIP3P potential.[22] A restraining potential was used at the solvent–vacuum boundary. The reaction field beyond the boundary was added to the simulation results as a correction term using FDP (see below). Similar protein regions were simulated with a GB model,[23] ASP[24] and a modeled linear distance-dependent protein dielectric constant ($\varepsilon = r$). For comparison purposes, a vacuum ($\varepsilon = 1$) calculation was performed.

Non-bonded interactions were calculated using a spherical cut-off of 20 Å. The protein dielectric constant (ε_p) was set to 1, and for the GB model 80 was used to model bulk water. Ionization states were set corresponding to a neutral pH. Starting velocities were assigned from a Boltzmann distribution at 298K. The integration timestep was set at 1.0 fs, and simulations were initiated with a 50 ps equilibration phase followed by a 500 ps production calculation, with a total of 1000 conformations culled from each simulation.

Conformational entropy was determined by solving eq. (10), using the solutions to the covariance fluctuation matrix. All heavy atoms of the active-site region were used in the evaluation of TS_{conf}.

The LRA model was solved with α and β set to 0.50 and 0.16, respectively.[9] Cavitation energies were determined from the molecular surface using the Connolly algorithm[25] with the solvent probe radius set at 1.4 Å. The numerical value of γ was defined as 69 cal mol^{-1} Å^{-2} for all atom types.[26] The vdW solvation free energy term for implicit solvent model calculations was scaled as $G_{\text{s,vdW}} \approx \mu G_{\text{cav}}$, where μ was determined from LRA.

The FDP method implemented was from the program DelPhi.[27] Electrostatic potentials for each molecule were calculated using molecular surfaces to define regions of low dielectric medium ($\varepsilon_p = 1$) embedded in high dielectric solvent water ($\varepsilon_w = 80$). DelPhi calculations were carried out on a cubic grid of resolution 0.6 Å/point, giving a total of 149^3 grid points. For the explicit solvent reaction-field correction term, waters were removed and the dielectric boundary approximated by scaling the atomic vdW radii of the protein to encapsulate the simulation volume, and a grid of 1.0 Å/point was applied. Full Coulombic boundary conditions were applied for all FDP calculations.

RESULTS AND DISCUSSION

Table I summarizes the free energy components of ΔG_{macro} determined for each of the simulation models. The reported errors reflect the statistical uncertainty in the sampling distributions and were evaluated as the standard deviation of the free energy divided by the square root of the sample size; namely, $Z(\sigma G_{\text{macro}})/\sqrt{N}$, where $Z = 1.6452$ is the number of standard deviations from the mean that is needed to claim with 95% confidence the value of the true mean. Convergence is an issue of all sampling problems, and while the simulation time and sample size of the calculations are moderate, the observed trends among the solvent models have converged.

The result of the explicit solvent simulation using the LRA to calculate the free energy difference yields a ΔG_{macro} of ≈5 kcal/mol and predicts stabilization of the 'in' state, which is consistent with the experimental estimate of $\Delta G_{\text{expt}} \approx 4$ kcal/mol.[1,3–7] Because of the complexity of isolating the effect of conformational change and its thermodynamic underpinning from the inhibitor reaction, ΔG_{expt} is a rough multipart estimate. Nevertheless, the proposal that the ΔG_{expt} is due primarily to structural reorganization is corroborated by site-directed mutagenesis of human AChE at residues Phe-295 and Phe-297 in the loop segment and the effect on binding DFP.[6,7] These two phenylalanines of AChE are conserved among species and are equivalent to Phe-288 and Phe-290 in *Torpedo* (see Fig. 1). Substituting both residues with smaller aliphatic side chains favorably alters the free energy of association for DFP by ≈4 kcal/mol and is similar to binding inhibitors

TABLE I. Summary of Energy Differences (kcal/mol) from Simulations Employing Different Solvent Models for (in → out) Loop Reorganization on Acetylcholinesterase*

ΔE_{np}	ΔW_{ele}	$\Delta G_{s,ele}$		$\Delta G_{s,vdW}$	ΔG_{cav}	$-T\Delta S_{conf}$	$\Delta G_{macro}^{in \rightarrow out}$
Explicit Solvent							
−1.2	−116.3	LRA	130.9	0.1	0.1	−8.3	5.3 ± 3.6
−1.2	−116.3	GB	123.7	0.1	0.1	−8.3	−1.9 ± 3.2
−1.2	−116.3	FDP	117.6	0.1	0.1	−8.3	−8.0 ± 3.4
GB/SA							
−2.9	−52.1	GB	63.6	0.1	0.1	−4.5	4.3 ± 3.2
−2.9	−52.1	FDP	56.0	0.1	0.1	−4.5	−3.3 ± 3.1
ASP							
−50.9	42.8	ASP	−19.3	0.1	0.1	−8.9	−36.1 ± 2.4
−50.9	42.8	GB	−46.7	0.1	0.1	−8.9	−63.5 ± 2.7
−50.9	42.8	FDP	−46.2	0.1	0.1	−8.9	−63.0 ± 2.6
$\varepsilon = r$							
34.1	−51.4	$\varepsilon = r$	0.0	0.1	0.1	−9.5	−26.6 ± 2.3
34.1	−128.2	GB	115.2	0.1	0.1	−9.5	11.8 ± 2.3
34.1	−128.2	FDP	101.6	0.1	0.1	−9.5	−1.8 ± 2.4
$\varepsilon = 1$							
−5.2	−36.0	GB	41.8	0.1	0.1	−14.1	−13.3 ± 2.0
−5.2	−36.0	FDP	36.7	0.1	0.1	−14.1	−18.4 ± 2.0

*Experimental estimate taken to be on the order of ~4 kcal/mol.[1,3–7] The term ΔE_{np} is defined as bonded and torsional terms plus internal vdW.

where no loop movement is observed crystallographically.[6,7] The simulation results of Table I support the view that the energetic cost is consequent of loop displacement.

Free energy terms ΔG_{cav} and $\Delta G_{s,vdW}$ are insignificant in discrimination between the two states, and ΔE_{exp} (bonded and torsional terms plus internal vdW) produces a small contribution that favors the 'out' macrostate. The dominant terms are the electrostatic compensation of ΔW_{ele} vs. $\Delta G_{s,ele}$, and conformational entropy. The latter reveals a topology of a wider 'out' basin and allows for greater dynamic connectivity among microstates.

The agreement obtained from the LRA model with the experimental estimate is encouraging from the perspective of not having to scale α in eq. (7) from the initial value of 0.5. Generally, for the application of LRA, the *a priori* determination of α clearly hinders its use, although if data are available, mutational free energies or ligand-binding affinities can be used to fit both scaling parameters of eq. (7).

The next computational approach is the rescoring of the MD trajectories by removing the explicit water and calculating the solvent polarization term with either the GB model or the Poisson equation. Table I shows that values of $\Delta G_{s,ele}$ for both implicit solvent models are underestimated in comparison with the LRA calculation. This is most evident for the more rigorous Poisson equation. The observed reduction in differentiation of solvent polarization between the macrosates is the outcome of transitioning conformations that were thermally equilibrated on an explicit solvent potential energy surface to a non-optimal implicit solvent environment. The solvent perturbation incorrectly alters the energy landscape without any conformational relaxation to adapt to the new topology. In other words, conformations culled at 298K in explicit solvent are positioned at a higher energy on the potential energy surface from changing to implicit solvent. Errors arise principally from charged residues (e.g., Arg-289), and the lack of cancellation of relative error in $\Delta G_{s,ele}$ is due to conformational dependence of the electric field. Reconciliation of the implicit solvent results by simple scaling the homogeneous ε_p to account for dipolar reorientation will fail to provide consistent improvement. As commented below, the calculations illustrate the difficulty of obtaining accurate and reliable results from the approach of rescoring conformations with a solvent model different from the one used to generate the ensemble.

The third set of calculations is the MD-GB/SA model simulations, which show accuracy in ΔG_{macro} comparable with that of the LRA. This result is promising, yet inspection of the electrostatic free energy terms reveals significant differences in sampling microstates. Conformations found from exploring the GB potential surface are optimized as a result of instantaneous solvent dipolar relaxation embedded in the mean-field approximation, while explicit water calculations treat dipolar reorientation. This distinction is apparent from scatter plots of FDP vs. GB (Fig. 2). Scoring conformations by FDP reveals roughly the same range of values as the ensemble generated from MD-GB/SA and from explicit water calculations, while scoring the MD-GB/SA ensemble by GB favors a shift on the order of 100 kcal/mol from the ideal correlation between GB and FDP. The latter is inconsistent with the explicit water results; the MD-GB/SA model simply searches for conformations optimized by an implicit reaction field. The strength of interaction between polarization charges of the protein and solvent scales as $(1/\varepsilon_p - 1/80)$ with the maximum value obtained for $\varepsilon_p = 1$ and charged residues in their ionized state. The indirect success of GB simulations without scaling the protein dielectric constant

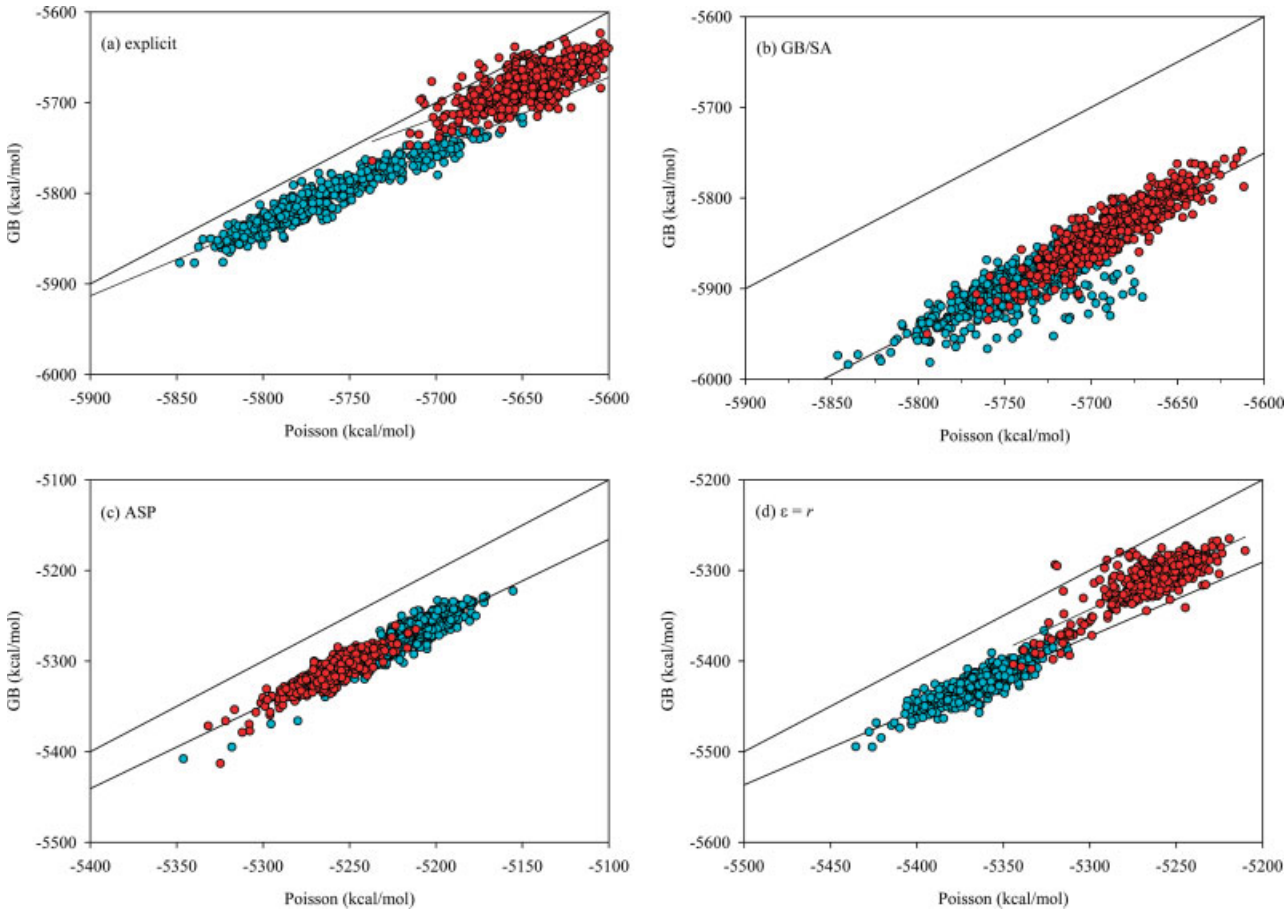

Fig. 2. Scatter plots of FDP vs. GB solvation free energies calculated from scoring molecular dynamics simulation trajectories using different solvent models. The basin of 'in' conformations is shown in blue and the 'out' in red. (a) Explicit solvent results; correlation coefficient (r^2) is 0.9 for the 'in' basin and 0.6 for the 'out.' (b) MD-GB/SA model; $r^2 = 0.8$ for both basins. (c) ASP solvent model; $r^2 = 0.9$ and 0.8 for the 'in' and 'out' conformations, respectively. (d) The $\varepsilon = r$ solvent model; $r^2 = 0.8$ and 0.7 for the 'in' and 'out' conformations, respectively. Each plot shows an ideal correlation and linear fits to the computed data.

is due to sufficient configurational averaging of the basins and their smooth-funnel topology.[18]

While the manifold of microstates sampled by the explicit solvent model and MD-GB/SA are different, similar results in ΔG_{macro} are predominantly due to the effect of the net electrostatic component on conformational sampling. From the explicit water simulation, $\Delta W_{\text{ele}} + \Delta G_{\text{s,ele}} =$ 14.6 kcal/mol, while from the MD-GB/SA, the sum equals 11.5 kcal/mol. The two simulation models show similar trends, whereas models of rescoring conformations either underestimate or failed to properly offset Coulombic charging by solvation. Again this supports the notion of obtaining self-consistency between generating ensembles and scoring them.

The overall scatter from a perfect linear fit of FDP vs. GB reflects insufficient parameterization of earlier GB models[23] for protein simulations and can be improved with more recent models.[28] For the explicit solvent calculations, the correlation coefficient is 0.9 for the 'in' macrostate and 0.6 for the 'out', while GB simulation yields 0.8 for both macrostates.

From Table I, the ASP model and the distance-dependent screening of charges are unsuccessful at producing accurate results. Both models show significant protein distortions reflected in ΔE_{np} and are no more reliable than vacuum calculations. Other modeling studies have noted protein distortions that result from using similar solvent models.[29] Despite the excellent agreement between GB and FDP for revaluating the trajectories generated by the ASP model (Fig. 2), the calculations show that the 'out' basin is more favorable by >60 kcal/mol. In comparison, dielectric screening correctly discriminates the 'in' basin by GB evaluation, yet consistent scoring by the function used to generate the ensemble fails. Incorrect modeling of solvent polarization and conformational distortions renders both models poor choices for sampling microstates.

ACKNOWLEDGMENTS

The author thanks Dr. L. Carlacci for computational assistance in the early stages of this work, Dr. M. Lee for many valuable discussions on the generalized Born model and Dr. C. B. Millard for suggesting the problem of acetylcholinesterase. This work was supported by the Army Medical Research and Materiel Command Project number RIID 02-4-1R-069. Opinions, interpretations, con-

clusions and recommendations are those of the author and are not necessarily endorsed by the U.S. Army.

REFERENCES

1. Millard CB, Kryger G Ordentlich A, Greenblatt HM, Harel M, Raves ML, Segall Y, Barak D, Shafferman A, Silman I, Sussman JL. Crystal structures of aged phosphonylated acetylcholinesterase: nerve agent reaction products at the atomic level. Biochem 1999;38:7032–7039.
2. Millard CB, Koellner G, Ordentlich A, Shafferman A, Silman I, Sussman JL. Reaction products of acetylcholinesterase and VX reveal a mobile histidine in the catalytic triad. J Am Chem Soc 1999;121:9883-9884.
3. Chiu YC, Main AR, Dauterman WC. Affinity and phosphorylation constants of a series of O,O-dialkyl malaoxons and paraoxons with acetylcholinesterase. Biochem Pharmacol 1969;18:2171–2177.
4. Hart GJ, O'Brien RD. Recording spectrophotometric method for determination of dissociation and phosphorylation constants for the inhibition of acetylcholinesterase by organophosphates in the presence of substrate. Biochem 1973;12:2940–2945.
5. Forsberg A, Puu G. Kinetics for the inhibition of acetylcholinesterase from the electric eel by some organophosphates and carbamates. Eur J Biochem 1984;140:153–156.
6. Ordentlich A, Barak D, Kronman C, Flashner Y, Leitner M, Segall Y, Ariel N, Cohen S, Velan B, Shafferman A. Dissection of the human acetylcholinesterase active center determinants of substrate specificity. Identification of residues constituting the anionic site, the hydrophobic site, and the acyl pocket. J Biol Chem 1996;268:17083–17095.
7. Ordentlich A, Kronman C, Barak D, Stein D, Ariel N, Marcus D, Velan B, Shafferman A. Engineering resistance to 'aging' of phosphylated human acetylcholinesterase. Role of hydrogen bond network in the active center. FEBS Lett 1993;334:215–220.
8. Muegge I, Schweins T, Warshel A. Electrostatic contributions to protein-protein binding affinities: application to Rap/Raf interaction. Proteins 1998;30:407–423.
9. Sham YY, Chu ZT, Tao H, Warshel A. Examining methods for calculations of binding free energies: LRA, LIE, PDLD-LRA, and PDLD/S-LRA calculations of ligands binding to an HIV protease. Proteins 2000;39:393–407.
10. Warshel A, Russel ST. Calculations of electrostatic interactions in biological systems and in solutions. Q Rev Biophys 1984;17:283–421.
11. Olson MA. Calculations of free energy contributions to protein-RNA complex stabilization. Biophys J 2001;81:1841–1853.
12. Dill KA. Polymer principles and protein folding. Protein Sci 1999;8:1166–1180.
13. Vorobjev YN, Almagro JC, Hermans J. Discrimination between native and intentionally misfolded conformations of proteins: ES/IS, a new method calculating conformational free energy that uses both dynamics simulations with an explicit solvent and an implicit solvent continuum model. Proteins 1998;32:399–413.
14. Amadei A, Linsen ABM, Berendsen HJC. Essential dynamics of proteins. Proteins 1993;17:412–425.
15. Brooks BR, Janezic D, Karplus M. Harmonic analysis of large systems. I. Methodology. J Comp Chem 1995;16:1522–1542.
16. Janezic D, Brooks BR. Harmonic analysis of large systems. II. Comparison of different protein models. J Comp Chem 1995;16:1543–1553.
17. Janezic D, Venable RM, Brooks BR. Harmonic analysis of large systems. III. Comparison with molecular dynamics. J Comp Chem 1995;16:1554–1566.
18. Carlacci L, Millard CB, Olson MA. Conformational energy landscape of the acyl pocket loop in acetylcholinesterase: A Monte Carlo-generalized Born model study. Biophys Chem 2004, In press.
19. Štrajbl M, Shurki A, Warshel A. Converting conformational changes to electrostatic energy in molecular motors: the energetics of ATP synthase. Proc Natl Acad Sci USA 2003;25:14834–14839.
20. Ponder JW. Tinker. Software for molecular design. Version 4.0, February 2003.
21. Cornell WD, Cieplak P, Bayly CI, Gould IR, Merz KM Jr., Ferguson DM, Spellmeyer DC, Fox T, Caldwell JW, Kollman PA. A second generation force field for the simulation of proteins, nucleic acids, and organic molecules, J Am Chem Soc 1995;117:5179–5197.
22. Jorgensen WL, Chandrasekhar J, Madura JD, Impey RW, Klein ML. Comparison of simple potential functions for simulations of liquid water. J Chem Phys 1983;79:926–935.
23. Qiu D, Shenkin PS, Hollinger FP, Still WC. The GB/SA continuum model for solvation. A fast analytical method for the calculation of approximate Born radii. J Phys Chem A 1997;101:3005–3014.
24. Eisenber D, McLachlan AD. Solvation energy in protein folding and binding. Nature 1986;319:199–203.
25. Connolly ML. Analytical molecular surface calculation. J Appl Cryst 1983;16:548–558.
26. Jackson RM, Sternberg MJE. Application of scaled particle theory to model the hydrophobic effect: implications for molecular association and protein stability. Protein Eng 1994;7:371–383.
27. Gilson MK, Hongi B. Calculation of the total electrostatic energy of a macromolecular system: solvation energies, binding energies, and conformation analysis. Proteins 1988;4:7–18.
28. Lee MS, Salsbury FR Jr., Brooks CL III. Novel generalized Born methods. J Chem Phys 2002;116:10606–10614.
29. Calimet N, Schaefer M, Simonson T. Protein molecular dynamics with the generalized Born/ACE solvent model. Proteins. 2001;45:144–158.